Guest Exchange with *n*-Alkanes and Host−Guest Interactions in the Clathrate Phase of Syndiotactic Polystyrene

Yukihiro Uda, Fumitoshi Kaneko,* and Tatsuya Kawaguchi

Department of Macromolecular Science, Graduate School of Science, Osaka University, Toyonaka, Osaka 560-0043, Japan

Received November 5, 2004; Revised Manuscript Received February 25, 2005

ABSTRACT: The influence of guest size on the guest exchange behavior of the δ form of syndiotactic polystyrene was investigated using a series of *n*-alkanes from *n*-hexane to *n*-decane as a guest. The bands due to sorbate and desorbate molecules and the conformational sensitive bands of sPS were followed by ATR-FTIR spectroscopy. The guest exchange of the δ form containing chloroform proceeded smoothly for all *n*-alkanes, but it became slow with the length of *n*-alkane. Although the amount of TTGG helices characteristic of the clathrate structure was kept during the exchange with *n*-hexane and *n*-heptane, a decrease in conformational regularity was observed in the beginning of the guest exchange of longer *n*-alkanes. The absorbed amount of *n*-alkanes decreased with the amount of the TTGG helices. The frequency shift of the methyl asymmetric stretching band of *n*-alkanes suggested that the packing of *n*-alkane molecules in the cavity became tight as the chain length increased.

Introduction

Since the synthesis of syndiotactic polystyrene (sPS) was reported,[1] a large amount of work has been focused on the complex polymorphic behavior of this polymer. At least four crystalline phases have been identified: α and β forms containing planar zigzag chains[2−7] and γ and δ forms containing helical chains of TTGG conformation.[8−11] The δ form is a clathrate compound, where small molecules are included in the cavities between polymer helices.[8−10] A porous crystalline phase named the δ_e form is obtained by extracting guest molecules from the δ form.[11,12] The cavities of the δ_e form can capture specific solvent molecules from solvent mixtures.[13−15] For example, the preferential absorption of chlorinated hydrocarbons into the δ_e form was confirmed in an aqueous solution of 1,2-dichloroethane and an acetone solution of chloroform.[13,16] The attractive interactions between chlorine atoms and phenyl groups of sPS have been demonstrated by FTIR spectroscopy[17] and molecular mechanics calculations.[14] The shape of guest molecules also affects its uptake into the δ_e form.[18−20] It is considered that the δ_e form has great potential in chemical separation and sensing devices.[13,15]

Recently, it has been clarified that the cavity of the δ form has another interesting property. The guest molecule in the δ form can be easily exchanged with another kind of molecule when the δ form is exposed to its vapor or soaked into its liquid.[21−24] The replacement of guest molecules is appreciably fast. For example, most toluene molecules stored in a film 2 μm thick are replaced with chloroform molecules within 1 min. Moreover, relatively large molecules such as *n*-decane, which cannot be included in the δ form by casting method, can be incorporated into the δ form using a guest exchange technique.[24] Recently, sophisticated utilization of sPS by incorporation of functional molecules into the δ form was proposed.[24] The guest exchange phenomenon would become an effective tool to construct composite materials of sPS with functional molecules.

* Corresponding author: e-mail toshi@chem.sci.osaka-u.ac.jp; Tel +81-6-6850-5453; Fax +81-6-6850-5288.

The guest exchange mechanism has not been studied in detail. It has been shown that the guest exchange behaviors, such as guest exchange rates and structural changes of sPS helices, depend on the combination of sorbate and desorbate molecules.[22] It is important to clarify the factors that dominate the guest exchange process of the δ form for the establishment of a new composite material formation method. In this study, we investigate the size effect of sorbate molecules using a series of *n*-alkanes from *n*-hexane to *n*-decane. It seems that there is no specific interactions between *n*-alkanes and sPS. Hence, the guest size effect may be separated from the other factors.

In this paper, we describe the absorption behavior of *n*-alkanes into a film of the δ form followed by FTIR-ATR spectroscopy, which provides information about not only variations in sorbate and desorbate concentrations but also conformational changes of sPS chains. We will demonstrate how the molecular size of *n*-alkanes affect the exchange rate, the amount of guest absorbed, and the conformational regularity of sPS.

Experimental Section

Samples. Syndiotactic polystyrene (sPS) was kindly supplied by Idemitsu Petrochemical Co., Ltd. The weight-average molecular weight was M_w = 197 000 (M_w/M_n = 1.98). Atactic polystyrene (aPS) was purchased from Aldrich Chemical Co. Its weight-average molecular weight was M_w = 280 000. Chloroform and *n*-alkanes (from *n*-hexane to *n*-decane) were purchased from Nakalai Tesque and used without further purification. Film samples of the δ form were prepared by spin-coating of sPS/chloroform solution onto an internal reflection element (IRE) of KRS-5. The film thickness was 2−3 μm, which was determined by comparing the absorbance of the 1601 cm^{-1} band in the transmission FTIR spectrum with that of the free-standing films of known thickness. Samples for thermogravimetiric analysis were prepared by immersing 50 μm thick films of the δ form into each *n*-alkane for more than 3 days. After this procedure, the films showed no IR bands due to chloroform. Each sample were kept for 24 h under vacuum before thermogravimetic analysis.

ATR-FTIR Measurements. ATR-FTIR spectra were taken with a BIO-RAD FTS-60A spectrometer equipped with a MCT detector at a resolution of 2 cm^{-1}. The IRE of KRS-5 with a

10.1021/ma047723d CCC: $30.25
Published on Web 03/25/2005

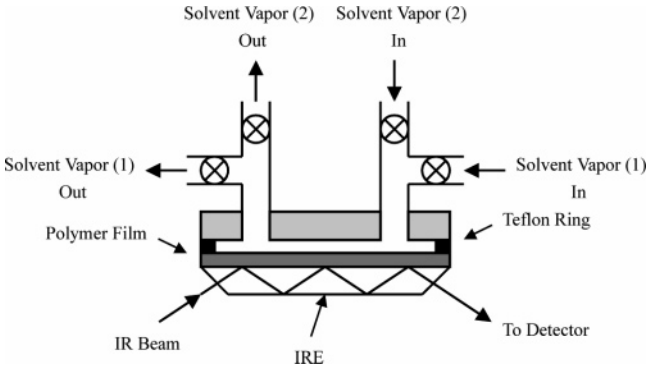

Figure 1. Schematic of the apparatus for ATR-FTIR measurement.

60° bevel was used. The apparatus used is illustrated in Figure 1. In this experimental condition, the penetration depth, which is usually used as a measure of effective measuring region, is about 0.5−2 μm from the interface between a polymer film and an IRE depending on the wavenumber of IR radiation. Since the density ratio of sPS to solvent vapor is about 1000:1, the contribution of molecules in the gas phase to an ATR-FTIR spectrum is negligible, even if a part of IRE is not covered with an sPS film and touched directly by solvent vapor. The details of this apparatus and the procedures for measuring guest exchange process were previously described.[21] Until the start of the exposure to a *n*-alkane vapor, a specimen was kept in the vapor of chloroform to prevent the desorption of chloroform from the specimen. IR spectra were taken at 1 s intervals with four scans during the first 3 min of the experiment and subsequently at 15 min intervals with 64 scans.

X-ray Diffraction Measurements. Powder X-ray diffraction diagrams were measured using a Rigaku RINT-2200 diffractometer with Cu Kα radiation (40 kV and 40 mA). The data were collected over the 2θ range from 5° to 40° at a rate of 0.5°/min with a step size of 0.05°.

Thermogravimetric Analysis. To obtain the concentration of *n*-alkane from ATR-FTIR spectra, it is necessary to measure the absorption intensities of *n*-alkane bands for a sample of known composition. For this purpose, thermogravimetric analysis was carried out for each sPS/*n*-alkane clathrate film using a Seiko SSC/5200 in the range 20−250 °C, with a scanning rate of 5 °C/min. The weight fractions of *n*-alkanes from *n*-hexane to *n*-decane were 0.083, 0.078, 0.072, 0.071, and 0.076, respectively.

The concentration of *n*-alkane in the film was evaluated from ATR spectra using the following equation

$$\bar{A} = \alpha \frac{d_{\text{alkane}}}{d_{\text{polymer}}} \frac{1 - \exp(-2L/d_{\text{alkane}})}{1 - \exp(-2L/d_{\text{polymer}})} C$$

where $\bar{A}$ is the absorbance ratio of the methyl asymmetric stretching [$\nu_a(CH_3)$] band of *n*-alkane to the sPS phenyl ring C=C stretching [$\nu(CC)_{ph}$] band at 1601 cm^{-1}, C is the concentration ratio of *n*-alkane to sPS, α is the absorption coefficient ratio of the $\nu_a(CH_3)$ band to the $\nu(CC)_{ph}$ band, and d_{alkane} and d_{polymer} are the penetration depths for the $\nu_a(CH_3)$ and $\nu(CC)_{ph}$ bands, respectively. The value of α was determined from the $\bar{A}$ and C values of the sample used for thermogravimetric analysis.

Results and Discussion

Guest Exchange Processes with *n*-Alkanes. Figure 2a shows the ATR-FTIR spectral changes of the δ form film containing chloroform on exposure to *n*-hexane vapor. Just after the initiation of the exposure, the band at 2956 cm^{-1} due to the methyl asymmetric stretching [$\nu_a(CH_3)$] of *n*-hexane[25,26] increased in intensity, while the band at 1219 cm^{-1} due to the C−H deformation [ν_4-($CHCl_3$)] of chloroform[27] decreased in intensity. On the other hand, the bands due to sPS did not show clear changes. For example, the intensities of the three bands due to TTGG sequences at 571, 548, and 501 cm^{-1} remained almost unchanged.[28−30] These spectral changes mean that the chloroform molecules in this film were replaced with *n*-hexane molecules, keeping the TTGG helices of sPS. Figure 3a shows the time dependence of the intensities of $\nu_a(CH_3)$, $\nu_4(CHCl_3)$, and the TTGG bands at 571 and 548 cm^{-1}. Within the first 6 s, about 80% of the intensity changes of the hexane and chloroform bands was completed, and only slight changes were observed after a lapse of 1 min. On the contrary, the intensities of the TTGG bands were constant during the whole process.

When exposed to *n*-decane vapor, the δ-form film showed similar but somewhat different spectral changes, as shown in Figures 2b and 3b. The intensity increase of the $\nu_a(CH_3)$ band of *n*-decane[25] and the intensity decrease of the $\nu_4(CHCl_3)$ band started immediately after the initiation of the exposure as is the case for *n*-hexane, but these spectral changes proceeded slower than those observed on the exposure to *n*-hexane. Gradual intensity changes continued even after 1 min from the inception. Furthermore, the intensity increase of the $\nu_a(CH_3)$ band of *n*-decane was rather small compared with that of *n*-hexane. Contrary to the exposure to *n*-hexane, a clear drop in intensity was observed in the bands due to the TTGG sequences in the 500−600 cm^{-1} region for 10 min from the inception. These differences in spectral changes suggest that the chain length of *n*-alkanes affects not only the sorption and desorption rates of *n*-alkane and chloroform but also the absorbed amount of *n*-alkane and the conformational regularity of sPS TTGG helices.

Such influence of *n*-alkane chain length is clearly seen in Figure 4. Although the exchange of *n*-alkane molecules with chloroform was observed in all cases, the following spectral differences concerning the absorption rate and absorbed amount of *n*-alkanes and the conformational regularity of sPS were observed. (1) The rate of intensity change of the $\nu_a(CH_3)$ band in the first 0.1 min decreased with an increase in chain length. Although the intensity change was almost completed in the first 1 min for *n*-hexane and *n*-heptane, a slow increase continued for longer *n*-alkanes. (2) The intensity of the $\nu_a(CH_3)$ band in the final stage (about 4 days after) decreased as the chain length increased. (3) The intensity of the conformational regularity band of sPS helices decreased on the guest exchange process for longer *n*-alkanes. The intensities of the TTGG bands at 571 and 548 cm^{-1} remained almost unchanged for *n*-hexane and *n*-heptane, but they showed a decrease in the first 10 min and a slow slight recover for *n*-octane, *n*-nonane, and *n*-decane.

Despite the above differences in spectral change, it is inferred that the absorbed *n*-alkane molecules are encapsulated into the cavities in the δ form for all cases for the three reasons below. First, the powder X-ray diffraction diagram of the film whose original guest chloroform was replaced with *n*-decane or *n*-hexane showed a distinct peak due to the $\bar{2}10$ reflection at $2\theta \approx 10.2°$, which is extinct without guest molecules for the clathrate phase of sPS,[11] as well as the δ form containing chloroform, as shown in Figure 5. Furthermore, the relative intensity of the 20° peak to the 17° peak is different between δ(chloroform), δ(*n*-hexane),

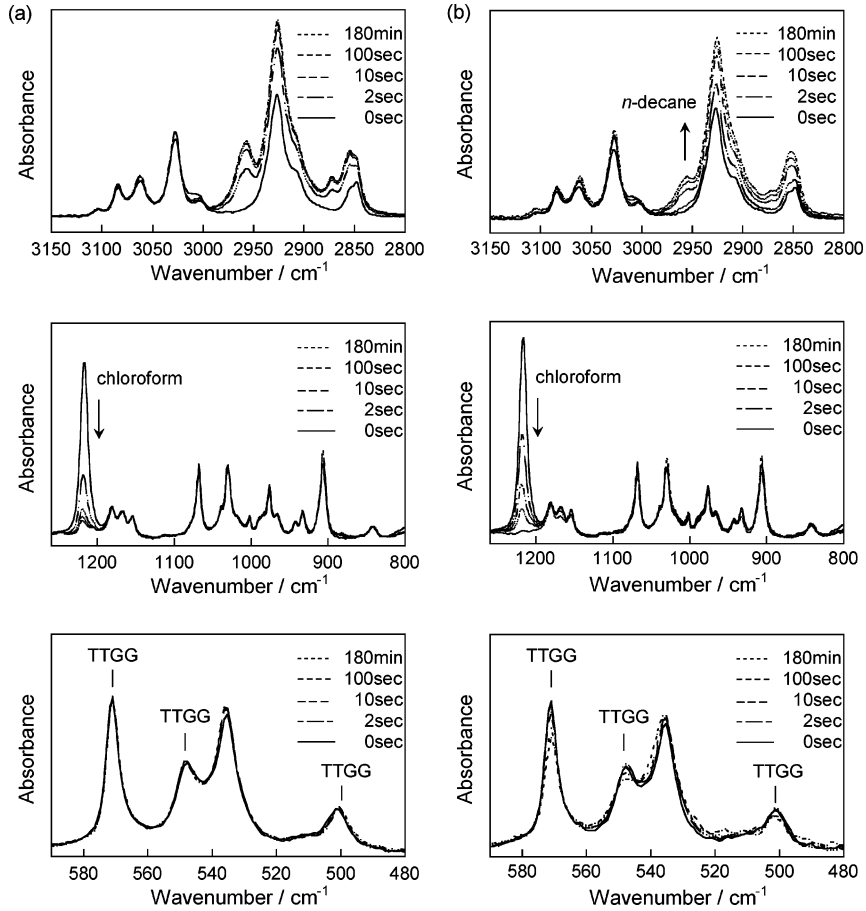

Figure 2. FTIR-ATR spectral changes of the δ form including chloroform as a guest on exposure to *n*-alkane vapor: (a) *n*-hexane and (b) *n*-decane.

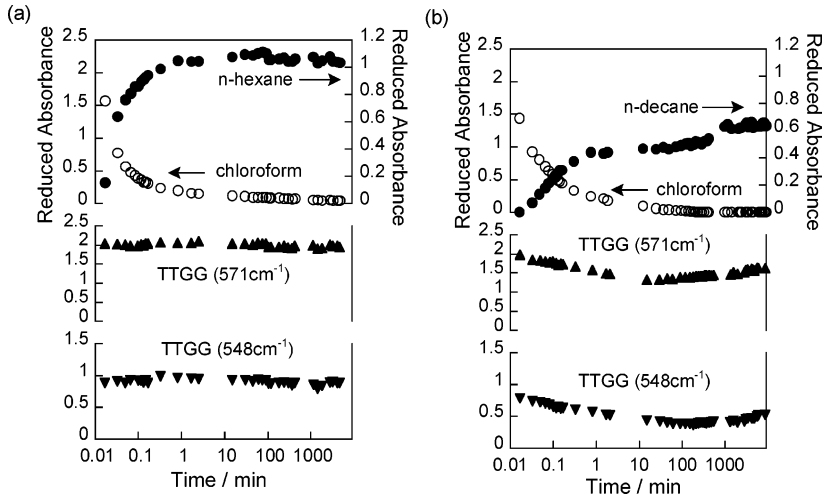

Figure 3. Variation in the absorbance for the 1219 cm^{-1} chloroform C−H deformation band, the 2956 cm^{-1} methyl asymmetric stretching of *n*-alkane band, and the TTGG bands at 548 and 571 cm^{-1} during the exposure of the δ form to *n*-alkane vapor: (a) *n*-hexane and (b) *n*-decane. To correct the intensity difference between samples due to irreproducible sample contact with the IRE, the absorbance of each band was reduced using the phenyl ring band at 1601 cm^{-1} as the internal standard.

and δ(*n*-decane); such variation in X-ray profile is observed when the guest is exchanged.[31] Second, the solubility of *n*-alkane molecules into the amorphous region of sPS is rather low and decreases rapidly with the chain length. For example, contrary to chloroform that swells sPS soon, *n*-decane does not make sPS swollen. No distinct IR bands due to *n*-decane were observed for an sPS glass film immersed in *n*-decane for 10 days. Third, the relative amount of *n*-alkane to sPS in the final stage was nearly proportional to the fraction of TTGG sequences of sPS, which will be described in detail in the next section.

Accordingly, the intensity of the $\nu_a(CH_3)$ band can be used as a measure of the amount of *n*-alkanes stored in the clathrate structure of sPS. On the basis of the spectral data, the guest exchange behavior of each *n*-alkane molecule can be described as follows. For *n*-hexane and *n*-heptane, a smooth guest exchange takes place without large destruction of the TTGG helices. However, as the *n*-alkane length increases, the guest

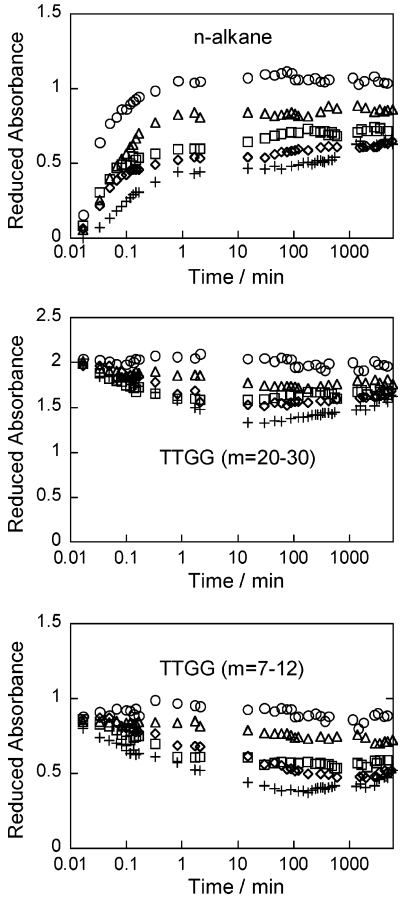

Figure 4. Variation in the reduced absorbance for *n*-alkane, TTGG ($m = 20-30$), and TTGG ($m = 7-12$) bands during the exposure of the δ form to *n*-alkane vapor: *n*-hexane (○), *n*-heptane (△), *n*-octane (□), *n*-nonane (◇), and *n*-decane (+).

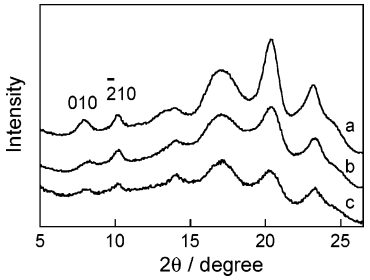

Figure 5. X-ray diffraction patterns of the δ-form samples including different guests: (a) *n*-hexane, (b) *n*-decane, and (c) chloroform.

exchange proceeds slowly, accompanying a certain extent of conformational disordering of the TTGG helices, which causes a decrease in the absorbed amount of *n*-alkanes. Very slow re-formation of the TTGG helices also takes place, incorporating *n*-alkane molecules into the cavities; in particular, the re-formation is prominent on the exposure to *n*-decane.

Analysis of TTGG Conformation Bands. As described above, the absorbed *n*-alkane molecules affected the conformational regularity of sPS chains in the resultant films. Figure 6a shows the IR spectra of the δ-form films containing *n*-hexane and *n*-decane as a guest. The intensity decrease observed in the TTGG bands at 571, 548, and 501 cm^{-1} shows the lowering of conformational regularity in the δ-form film containing *n*-decane. Since IR bands of polymers have their own sensitivity to the conformational regularity, a more detailed pictures about the structural change of the sPS chain can be obtained by analyzing the intensity variation of each IR band.

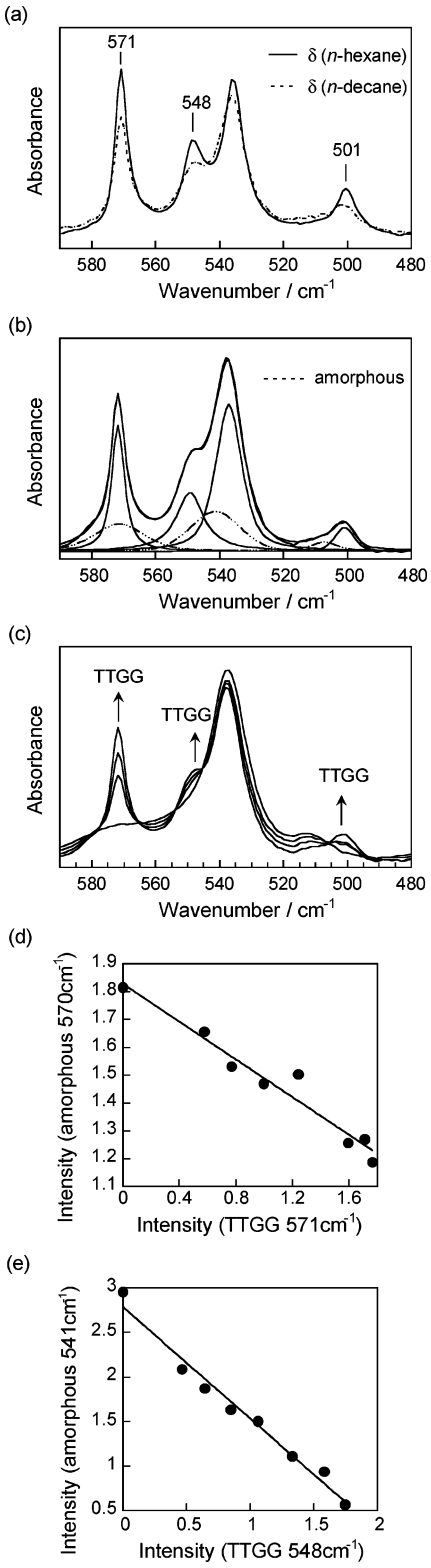

Figure 6. (a) IR spectra of the δ form of sPS including *n*-hexane and *n*-decane as a guest. (b) An example of curve fitting of the δ form. (c) IR spectral change of the glass sample during the solvent-induced crystallization. (d) A plot of A_{amor} at 570 cm^{-1} against A_{TTGG} at 571 cm^{-1} obtained at various times during the solvent-induced crystallization of the glass sample. (e) A plot of A_{amor} at 541 cm^{-1} against A_{TTGG} at 548 cm^{-1} obtained at various times during the solvent-induced crystallization of the glass sample.

The sensitivity of the conformation regularity band can be assessed quantitatively with a concept of critical sequence length (CSL), which is defined as the shortest length of the sequence of a particular conformation necessary for the appearance of the band and represented by the number of monomeric residues m constituting the sequence.[32] The values of CSL for the TTGG bands in Figure 6a were evaluated as follows: 571 cm^{-1} ($m = 20-30$), 548 cm^{-1} ($m = 7-12$), and 501 cm^{-1} ($m = 12-20$).[33]

The IR spectra of the δ form in the region from 480 to 590 cm^{-1} can be decomposed into several bands, as shown in Figure 6b. There are three amorphous bands at 570, 541, and 507 cm^{-1} appearing near the TTGG bands.[33-35] Figure 6c shows the FTIR spectral change on the solvent-induced crystallization process of the glass sample of sPS. Isosbestic points were observed around every TTGG band, which suggests that the conformational ordering can be regarded as a two-component reaction from the disordered state (amorphous) to the ordered state (δ form).[36] The following equations can be applied to this two-component system according to Lambert−Beer's law:

$$A_{amor} = \epsilon_{amor} C_{amor} l \tag{1}$$

$$A_{TTGG} = \epsilon_{TTGG} C_{TTGG} l \tag{2}$$

where A_i ϵ_i, and C_i are the absorbance, the molar extinction coefficient, and the molar concentration of component i (i = amorphous and TTGG), and l is the optical path length. Since $C_{amor} + C_{TTGG} = 1$, the following equation is obtained:

$$A_{amor} = -\left(\frac{\epsilon_{amor}}{\epsilon_{TTGG}}\right) A_{TTGG} + \epsilon_{amor} l \tag{3}$$

A plot of A_{amor} against A_{TTGG} gives a straight line with a slope of $-(\epsilon_{amor}/\epsilon_{TTGG})$, as shown in Figure 6d,e. From these plots, $\epsilon_{amor}/\epsilon_{TTGG}$ for the 571 cm^{-1} TTGG ($m = 20-30$) and 570 cm^{-1} amorphous bands was estimated as 0.339 and that for the 548 cm^{-1} TTGG ($m = 7-12$) and 541 cm^{-1} amorphous bands as 1.25. Using the values of $\epsilon_{amor}/\epsilon_{TTGG}$ thus obtained, we can evaluate the molar fraction x_{TTGG} of the TTGG sequences equal to or longer than the CSL according to the equation[34]

$$\frac{1}{x_{TTGG}} = 1 + \frac{A_{amor}}{A_{TTGG}} \frac{\epsilon_{TTGG}}{\epsilon_{amor}} \tag{4}$$

The evaluated x_{TTGG} for large CSL ($m = 20-30$) and small CSL ($m = 7-12$) at the final stage of this experiment (about 10 000 min) were plotted against the number of carbon atoms of guest n-alkanes in Figure 7. The values of x_{TTGG} for each CSL decreased with the increase in the number of carbon atoms of guest n-alkanes. Especially, the x_{TTGG} value for the small CSL decreased greatly compared to that for the long one. All TTGG sequences consisting of not less than 7−12 monomers, namely most TTGG helices, contribute to the intensity of the 548 cm^{-1} TTGG band with small CSL, whereas only TTGG sequences consisting of not less than 20−30 monomers contribute to the intensity of the 571 cm^{-1} TTGG band with large CSL. Therefore, the result summarized in Figure 7 means that TTGG helices, in particular short TTGG helices, become disordered as the length of the sorbate n-alkane increases.

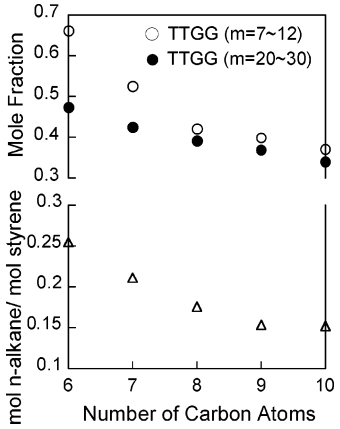

Figure 7. Mole fractions of TTGG helices and the concentration of n-alkanes in the δ form plotted against the number of carbon atoms of n-alkanes.

As for n-alkanes longer than n-heptane, most of the remaining TTGG helices in the final stage are long TTGG helices, as shown in Figure 7. In other words, the ability to form the clathrate phase with large guest molecules is larger for long TTGG helices. The tendency that short TTGG sequences became disordered was also observed on the exposure of a film containing toluene as a guest to chloroform vapor.[21]

Peak Shifts of *n*-Alkanes in the *δ* Form. The encapsulation into the cavities of sPS brings about a low-frequency or high-frequency shift in some vibrational modes. For example, 1,2-dichloropropane shows a low-frequency shift of the C−Cl stretching mode on the transfer from amorphous to crystalline region,[17] but 1,2-dichloroethane shows a high-frequency shift of this mode.[20]

On the contrary, the methyl asymmetric stretching $\nu_a(CH_3)$ mode showed only an low-frequency shift for all n-alkanes from n-hexane to n-decane. The frequency shift of the $\nu_a(CH_3)$ mode had a dependence on chain length. The $\nu_a(CH_3)$ mode of n-hexane appeared at a 3 cm^{-1} higher frequency in the δ form than in atactic polystyrene (aPS), but there was no such a clear difference for n-decane (Figure 8b). The peak positions of n-alkanes included in sPS and aPS are shown in Figure 9. As the chain length of n-alkanes increased, the $\nu_a(CH_3)$ band shifted to lower frequencies in the δ form, while the peak position was constant in aPS.

There are different kinds of vibrational modes in the fingerprint region, and they are coupled with each others intricately. The complex frequency shift on clathration can be considered as a result of vibrational coupling changes caused by many factors, such as host−guest interaction, molecular deformation, and conformational change. On the other hand, the $\nu_a(CH_3)$ mode is a highly localized mode, and the frequency of the $\nu_a(CH_3)$ mode hardly depends on the conformational changes. Therefore, we infer that the shift of $\nu_a(CH_3)$ mode is attributable to the difference in the local environment of the methyl group. To introduce this effect, we adopt the simplest theoretical treatment of peak shift given by Kirkwood and by Bauer and Magat, known as the Kirkwood−Bauer−Magat (KBM) relationship

$$\frac{\Delta\nu}{\nu} = \frac{C(\epsilon - 1)}{2\epsilon + 1} \tag{5}$$

where ν is the vibrational frequency of the solute, ϵ is

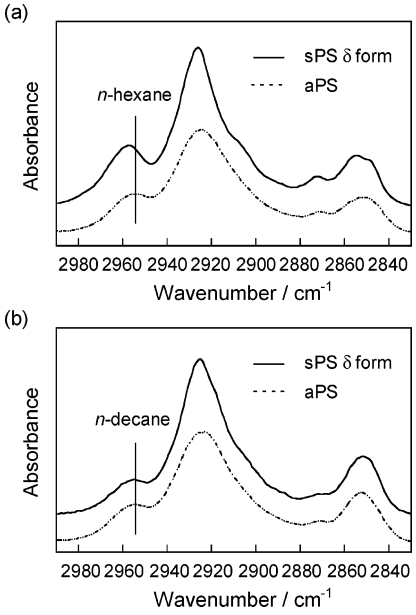

Figure 8. IR spectra of the δ form of sPS and aPS including different *n*-alkanes: (a) *n*-hexane and (b) *n*-decane.

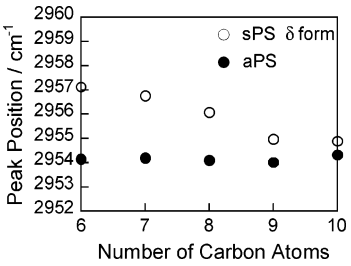

Figure 9. Peak positions of methyl asymmetric stretching bands of *n*-alkanes in the δ form of sPS and aPS.

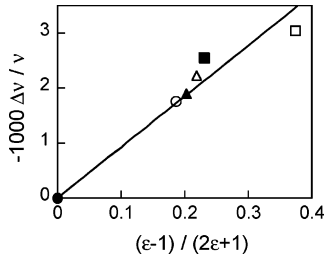

Figure 10. Kirkwood−Bauer−Magat plot of shifts in the methyl asymmetric stretching vibrational frequency of *n*-hexanes against dielectric constant. Solvents: *n*-hexane gas (●), *n*-hexane liquid (○), benzene (■), nitrobenzene (□), cyclohexane (▲), and decalin (△).

the dielectric constant of the solvent, and C is a constant for the solute vibrational mode.[37,38] Actually, the peak position of the $\nu_a(CH_3)$ band of *n*-hexane changes in the region of 2965−2954 cm^{-1}, depending on the surroundings of the CH_3 groups. The KBM plot for *n*-hexanes in gas and liquid phases is shown in Figure 10. $\Delta\nu/\nu$ is essentially proportional to $(\epsilon - 1)/(2\epsilon + 1)$.

On the basis of the above discussion, it is inferred that the difference in the immediate surroundings of the methyl group is the primary cause for the frequency difference of the $\nu_a(CH_3)$ mode between aPS and sPS and the characteristic low-frequency shift accompanied by the increase of *n*-alkane chain length in sPS. It seems that the most significant difference between aPS and sPS is the structural flexibility for the molecular size and shape of *n*-alkanes. The aPS chains in the amorphous region would change their shape according to the form of the sorbate *n*-alkane molecules and form a dense matrix having nearly the same structure, irrespective of the chain length of *n*-alkanes. Therefore, the local structure that the $\nu_a(CH_3)$ mode feels is expected to remain almost unchanged in increasing chain length from *n*-hexane to *n*-decane, which is consistent with the experimental result.

On the contrary, the cavity in the crystalline region of sPS has a definite shape: a space framed by 10 phenyl groups. The cavity volume can change to some extent,[39] but it is expected that changes in the shape and size of the cavity are small compared with those in the amorphous matrix of aPS, almost regardless of the size of the guest molecules. In other words, the cavity volume does not increase as much as the guest size. For the storage of *n*-hexane having a volume of 115 Å^3, the cavity of the δ form has enough room. However, *n*-alkanes will become packed more densely with increasing chain length, and the $\nu_a(CH_3)$ mode feels more strongly its surroundings, which causes the $\nu_a(CH_3)$ mode to shift to lower frequencies.

Conclusion

The effect of guest size on the guest exchange behavior of the δ form of sPS was investigated using a series of *n*-alkanes from *n*-hexane to *n*-decane as guest molecules. Although the exchange of chloroform with *n*-hexane or *n*-heptane proceeded keeping the TTGG conformation of sPS, a decrease in conformation regularity was observed on the exchange process of larger *n*-alkanes. The extent of disordering of TTGG helices was greater on shorter TTGG helices than longer ones. The frequency shift of methyl asymmetric stretching band of *n*-alkanes in the δ form suggested that the guest *n*-alkane become packed more tightly with increasing chain length.

Acknowledgment. The authors thank Idemitsu Petrochemical Co., Ltd., for supplying the sPS samples. They also thank Dr. Satoshi Kawata of Graduate School of Science of Osaka University for his help in the thermogravimetric analysis. The financial support of the Ogasawara Foundation for the Promotion of Science & Technology is also acknowledged. Y.U. expresses his special thanks for the Center of Excellence (21COE) program "Creation of Integrated EcoChemistry of Osaka University".

References and Notes

(1) Ishihara, N.; Seimiya, T.; Kuramoto, M.; Uoi, M. *Macromolecules* **1986**, *19*, 2464.
(2) Greis, O.; Xu, Y.; Asano, T.; Petermann, J. *Polymer* **1989**, *30*, 590.
(3) De Rosa, C.; Guerra, G.; Petraccone, V.; Corradini, P. *Polym. J.* **1991**, *23*, 1435.
(4) De Rosa, C. *Macromolecules* **1996**, *29*, 8460.
(5) Cartier, L.; Okihara, T.; Lotz, B. *Macromolecules* **1998**, *31*, 3303.
(6) De Rosa, C.; Rapacciuolo, M.; Guerra, G.; Petraccone, V.; Corradini, P. *Polymer* **1992**, *33*, 1423.
(7) Chatani, Y.; Shimane, Y.; Ijitsu, T.; Yukinari, T. *Polymer* **1993**, *34*, 1625.
(8) Chatani, Y.; Shimane, Y.; Inagaki, T.; Ijitsu, T.; Yukinari, T.; Shikuma, H. *Polymer* **1993**, *34*, 1620.
(9) Chatani, Y.; Shimane, Y.; Inagaki, T.; Shikuma, H. *Polymer* **1993**, *34*, 4841.
(10) De Rosa, C.; Rizzo, P.; De Ballesteros, O. R.; Petraccone, V.; Guerra, G. *Polymer* **1999**, *40*, 2103.
(11) De Rosa, C.; Guerra, G.; Petraccone, V.; Pirozzi, B. *Macromolecules* **1997**, *30*, 4147.

(12) Amutha Rani, D.; Yamamoto, Y.; Mohri, S.; Sivakumar, M.; Tsujita, Y.; Yoshimizu, H. *J. Polym. Sci., Part B: Polym. Phys.* **2003**, *41*, 269.
(13) Guerra, G.; Milano, G.; Venditto, V.; Lofferedo, F.; Ruiz de Ballesteros, O.; Cavallo, L.; De Rosa, C. *Macromol. Symp.* **1999**, *138*, 131.
(14) Guerra, G.; Milano, G.; Venditto, V.; Musto, P.; De Rosa, C.; Cavallo, L. *Chem. Mater.* **2000**, *12*, 363.
(15) Mensitieri, G.; Venditto, V.; Guerra, G. *Sens. Actuators B* **2003**, *92*, 255.
(16) Guerra, G.; Manfredi, C.; Musto, P.; Tavone, S. *Macromolecules* **1998**, *31*, 1329.
(17) Musto, P.; Manzari, M.; Guerra, G. *Macromolecules* **2000**, *33*, 143.
(18) Sivakumar, M.; Yamamoto, Y.; Amutha Rani, D.; Tsujita, Y.; Yoshimizu, H.; Kinoshita, T. *Macromol. Rapid Commun.* **2002**, *23*, 77.
(19) Daniel, C.; Alfano, D.; Guerra, G.; Musto, P. *Macromolecules* **2003**, *36*, 1713.
(20) Daniel, C.; Alfano, D.; Guerra, G.; Musto, P. *Macromolecules* **2003**, *36*, 5742.
(21) Yoshioka, A.; Tashiro, K. *Macromolecules* **2003**, *36*, 3593.
(22) Uda, Y.; Kaneko, F.; Kawaguchi, T. *Polymer* **2004**, *45*, 2221.
(23) Rizzo, P.; Della Guardia, S.; Guerra, G. *Macromolecules* **2004**, *37*, 8043.
(24) Uda, Y.; Kaneko, F.; Kawaguchi, T. *Macromol. Rapid Commun.* **2004**, *25*, 1900.
(25) Schachtschneider, J. H.; Snyder, R. G. *Spectrochim. Acta* **1963**, *19*, 117.
(26) Snyder, R. G. *J. Chem. Phys.* **1967**, *47*, 1316.
(27) Gibian, T. G.; McKinney, D. S. *J. Am. Chem. Soc.* **1951**, *73*, 1431.
(28) Kobayashi, M.; Nakaoki, T.; Ishihara, N. *Macromolecules* **1989**, *22*, 4377.
(29) Kobayashi, M.; Nakaoki, T.; Ishihara, N. *Macromolecules* **1990**, *23*, 78.
(30) Nyquist, R. A.; Putzig, C. L.; Leugers, M. A.; McLachlan, R. D.; Thill, B. *Appl. Spectrosc.* **1992**, *46*, 981.
(31) Chatani, Y.; Shimane, Y.; Inoue, Y.; Inagaki, T.; Ishioka, T.; Ijitsu, T.; Yukinari, T. *Polymer* **1992**, *33*, 488.
(32) Kobayashi, M.; Akita, K.; Tadokoro, H. *Macromol. Chem.* **1968**, *118*, 324.
(33) Tashiro, K.; Ueno, Y.; Yoshioka, A.; Kobayashi, M. *Macromolecules* **2001**, *34*, 310.
(34) Kobayashi, M.; Yoshioka, T.; Imai, M.; Itoh, Y. *Macromolecules* **1995**, *28*, 7376.
(35) Yoshioka, A.; Tashiro, K. *Macromolecules* **2004**, *37*, 467.
(36) Tashiro, K.; Ueno, Y.; Yoshioka, A.; Kaneko, F.; Kobayashi, M. *Macromol. Symp.* **1999**, *141*, 33.
(37) Kirkwood, J. G. *J. Chem. Phys.* **1938**, *4*, 592.
(38) Bauer, E.; Magat, M. *J. Phys. Radium* **1938**, *9*, 319.
(39) Milano, G.; Venditto, V.; Guerra, G.; Cavallo, L.; Ciambelli, P.; Sannino, D. *Chem. Mater.* **2001**, *13*, 1506.

MA047723D